High Magnetic Field and Magnetic Isotope Effects on Lifetimes of Triplet Biradicals Consisting of Two Equivalent Benzophenone Ketyls Linked by Methylene Chains

Yoshihisa Fujiwara, Takeshi Aoki, Takeharu Haino, Yoshimasa Fukazawa, and Yoshifumi Tanimoto*,†

Department of Chemistry, Faculty of Science, Hiroshima University, Kagamiyama, Higashi-Hiroshima 739, Japan

Ryoichi Nakagaki* and Osamu Takahira

Faculty of Pharmaceutical Sciences, Kanazawa University, Takara-Machi, Kanazawa 920, Japan

Masaharu Okazaki

National Industrial Research Institute of Nagoya, Hirate, Kita, Nagoya 462, Japan

Received: March 21, 1997; In Final Form: June 23, 1997[⊗]

External magnetic field and magnetic isotope effects on the lifetimes of several isotope-labeled triplet biradicals ($BPH^{\bullet}-O-(CH_2)_n-O-BPH^{\bullet}$, $n = 8$, 10, and 12) composed of two equivalent benzophenone ketyl radicals ($BPH^{\bullet}$s) were studied by laser flash photolysis in magnetic fields up to 14 T. The biradical lifetimes increased with increasing a magnetic field below *ca*. 3 T and then slightly decreased at 4−14 T. Below 4 T, a large magnetic isotope effect on the biradical lifetimes was observed in ^{13}C isotope substitution at a benzylic carbon of $BPH^{\bullet}$, whereas no magnetic isotope effect was observed above 4 T. The magnetic isotope effect in magnetic fields up to 4 T can be explained only by the spin−lattice relaxation mechanism due to the *anisotropic* hyperfine interaction of the biradicals.

1. Introduction

Magnetic field and magnetic isotope effects (MFEs and MIEs) on chemical reactions involving biradicals and radical pairs have been extensively studied over the past two decades.[1−7] Most of the research has been carried out in magnetic fields up to *ca*. 1 T with conventional electromagnets. Recently, we have found two new phenomena by combining a pulse magnet that can generate magnetic fields up to 14 T and a nanosecond laser flash photolysis apparatus.[8−10] The first is a reversal in biradical (radical pair) lifetimes with increasing magnetic fields.[8b−d,9] The second is the appearance of MIEs on the lifetimes even in high magnetic fields of 1−2 T and the disappearance of the MIEs in magnetic fields higher than 4 T.[10] The lifetimes of triplet biradicals derived from the photolysis of benzophenone$-CO_2-(CH_2)_{12}-O-$diphenylmethane (BP$-CO_2-(CH_2)_{12}-O-$DPM) and benzophenone$-CO_2-(CH_2)_{12}-O-$phenylethanol (BP$-CO_2-(CH_2)_{12}-O-$PET) have shown large MIEs in ^{13}C substitutions at their benzylic positions below 4 T; however, no MIE has been observed above 4 T.[10] The lifetimes at 1.5 T decreased from 9.9 to 7.7 μs and from 6.3 to 5 μs in the ^{13}C substitution in the respective radicals. To understand these phenomena in full detail, the following factors that may affect spin−lattice relaxation (SLR) processes should be quantitatively evaluated: anisotropic hyperfine and **g** tensors, rotational correlation times for the component radicals, and the magnitude of an electron dipole−dipole (dd) interaction between the radicals. By choosing appropriate radical structures, we can reduce the number of unknown parameters for those interactions. Triplet biradicals consisting of two equivalent benzophenone ketyl radicals ($BPH^{\bullet}$s) have been studied below 0.9 T by Nakagaki and his collaborators to avoid the complexity due to the difference in *g* values.[11] The biradical lifetimes below 0.9 T showed an increase in the lifetime with increasing magnetic fields, and a large MIE on the lifetime in the magnetic fields was observed in ^{13}C substitution at a benzylic position with the highest spin density in $BPH^{\bullet}$. They have interpreted the observed results in terms of the SLR mechanism. Useful information about the magnitude of magnetic interactions responsible for the SLR and rotational correlation times can be evaluated from the comparison between the biradical lifetimes obtained for the magnetic isotope species. If the decay process of the biradical in high magnetic fields is subject to an influence due to the anisotropic hyperfine (δhf) interaction that is dependent on nuclear spins, an MIE will be observed even in high magnetic fields. However, if the decay process is controlled by the dd interaction, such an MIE is unpredictable because the interaction is independent of nuclear spins. This paper presents the effects of high magnetic fields up to 14 T and magnetic isotopes on the dynamic behavior of the symmetric $BPH^{\bullet}-O-(CH_2)_n-O-BPH^{\bullet}$ biradicals.[12] Mechanisms for the MFE are discussed on the basis of the observed MIE.

2. Experimental Section

2.1. Materials. All compounds (BP-*n*-BH, $n = 8$, 10, and 12) (Chart 1) were available from the previous work.[11,13] The ^{13}C and ^{2}H isotope purities were *ca*. 99 and 98%, respectively. Spectrograde benzene (Wako) as a solvent was used without further purification. All sample solutions were degassed by several freeze−pump−thaw cycles. The concentration was adjusted to *ca*. 3×10^{-4} M.

2.2. Apparatus. Transient absorption signals were measured for biradical lifetime determination by a pulse magnet−laser flash photolysis apparatus.[8] In the laser flash photolysis, exciting and probe light sources were an excimer laser (Lumonics, EX-510) (308 nm, 15 ns fwhm, 30 mJ/pulse) and a Xe

* To whom correspondence should be addressed.
† E-mail: tanimoto@sci.hiroshima-u.ac.jp. Fax: ++81-824-24-7409.
⊗ Abstract published in *Advance ACS Abstracts,* August 1, 1997.

S1089-5639(97)01033-5 CCC: $14.00

CHART 1

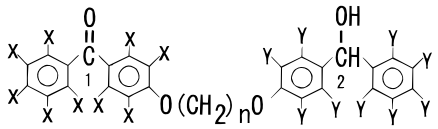

n=8, 10, 12

^{12}C-BP-n-BH-^{12}C: $C_1=C_2=^{12}C$, X=Y=^{1}H
^{13}C-BP-n-BH-^{12}C: $C_1=^{13}C$, $C_2=^{12}C$, X=Y=^{1}H
^{12}C-BP-n-BH-^{13}C: $C_1=^{12}C$, $C_2=^{13}C$, X=Y=^{1}H
^{13}C-BP-n-BH-^{13}C: $C_1=C_2=^{13}C$, X=Y=^{1}H
^{2}H-BP-12-BH-^{1}H: $C_1=C_2=^{12}C$, X=^{2}H, Y=^{1}H, n=12
^{1}H-BP-12-BH-^{2}H: $C_1=C_2=^{12}C$, X=^{1}H, Y=^{2}H, n=12
^{2}H-BP-12-BH-^{2}H: $C_1=C_2=^{12}C$, X=Y=^{2}H, n=12

arc lamp (Ushio, 150 W), respectively. The laser pulse and probe lights were introduced coaxially to a sample cell. The Xe light passed through a sample solution and was directed to a 20 cm monochromator (Ritsu, MC-20L)−photomultiplier (Hamamatsu, R636)−digital oscilloscope (Tektronix, 2440)−microcomputer (NEC, PC9801UV) detection system with a 0.8 mm i.d. quartz optical fiber (Sumitomo Electric Industries, MS-08).

2.3. Molecular Dynamics Simulation. An estimate of the mean inter-radical distance in the biradical was carried out by the mixed Monte Carlo/stochastic dynamics (MC/SD) method[14] using the MacroModel V5.0 program.[15,16] The MM3* force field was employed for the simulation with the GB/SA solvation model.[17] The total simulation time was 1000 ps with a 0.75 fs time step at 300 K for the SD part of the simulation. The MC part of the simulation used random rotations of all rotatable bonds. The ratio of SD steps to MC steps was 1-to-1. Nonbonded cutoff distances were not used. Structures were sampled every 1 ps for 1000 ps. The mean distance between the benzylic carbons in each BPH$^\bullet$ was evaluated from those sampled structures.

3. Results

3.1. Transient Absorption Spectra of BP-12-BH and Reaction Scheme. Figure 1 shows time-resolved transient absorption spectra generated from the photolysis of BP-12-BH in the absence and presence of a magnetic field (0.67 T). In the absence of a magnetic field, the spectrum at 0.60 μs showed absorption bands at 340, 540, and 650 nm. The spectra taken within 15 μs were the same as that observed at 0.60 μs. The spectrum at 90 μs had a peak at 320 nm. In the presence of a magnetic field (0.67 T), the spectra observed within 4 μs were identical with that observed at 0.60 μs in the absence of a magnetic field. At 11 μs, however, the spectra changed and a shoulder appeared at 350 nm.

For the purpose of comparison, transient absorption spectra generated from the photolysis of 4-dodecyloxybenzophenone (BP−O−$(CH_2)_{11}CH_3$) in benzene were examined, since a photoinduced intramolecular hydrogen abstraction (HA) reaction in this solution was considered to be inefficient. The transient spectra of BP−O−$(CH_2)_{11}CH_3$ had absorption bands at 340, 540, and 650 nm (lifetime = 8.4 ± 0.8 μs), which were assigned to the BP triplet−triplet absorption. In cyclohexane−benzene (1:1) mixed solvent, new peaks appeared at 345 and 560 nm with an intensity ratio of 1:0.15. They were assigned to BPH$^\bullet$−O−$(CH_2)_{11}CH_3$ because cyclohexane is a good hydrogen donor. Taking these spectra into account, the transient spectra shown in Figure 1 were assigned as follows. (i) The magnetic-field-independent spectra with the peaks at 340, 540, and 650 nm observed within 15 μs in the absence of a magnetic field were ascribed to the BP triplet−triplet absorption of BP-12-BH. (ii)

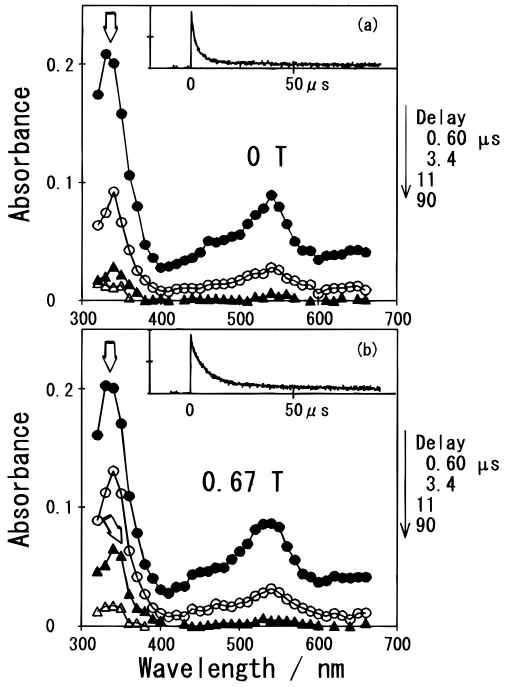

Figure 1. Time-resolved transient absorption spectra of ^{12}C-BPH$^\bullet$-12-BPH$^\bullet$-^{12}C in benzene at (a) 0 and (b) 0.67 T. Insets are the decay profiles monitored at 350 nm.

In the presence of a magnetic field, the spectra within 4 μs were also assigned to the BP triplet−triplet absorption of BP-12-BH by analogy. (iii) The magnetic-field-dependent shoulder at 350 nm observed at 11 μs was ascribed to BPH$^\bullet$−O−$(CH_2)_{12}$−O−BPH$^\bullet$ (BPH$^\bullet$−12−BPH$^\bullet$) generated from an intramolecular HA reaction of ^{3}BP* from BH at the other end of the methylene chain. Comparison of the lifetime (3.3 ± 0.3 μs) of ^{3}BP*-12-BH (see Table 1) with that (8.4 ± 0.8 μs) of ^{3}BP*−O−$(CH_2)_{11}$-CH_3 in benzene also indicates that intramolecular HA takes place in the former. It seems that the lifetime of BPH$^\bullet$-12-BPH$^\bullet$ in the absence of a magnetic field is short compared with that of ^{3}BP*-12-BH, since the steps in eqs 4 and 5 described later are estimated to be as fast as 10^7-10^8 s^{-1} and, experimentally, no detectable absorption band due to BPH$^\bullet$ was observed in the spectra in the absence of a magnetic field. On the other hand, the 320 nm band was tentatively attributed to reaction products because it remained even at 90 μs.

Based on the above-mentioned transient spectra and the reported photochemical process of BP and its derivative,[11,18] the reaction pathways of the BP-12-BH are given as follows. Upon 308 nm laser excitation of BP-*n*-BH (n = 8, 10, and 12) in benzene at room temperature, intramolecular HA takes place (eqs 1−3).[11,13] The ^{3}BP* abstracts a hydrogen atom from a benzylic position of BH to yield a triplet biradical composed of two equivalent BPH$^\bullet$s as shown in the following scheme:

$$\text{BP-}n\text{-BH} \xrightarrow{h\nu\ 308\ \text{nm}} {}^1\text{BP*-}n\text{-BH} \quad (1)$$

$${}^1\text{BP*-}n\text{-BH} \xrightarrow{\text{ISC}} {}^3\text{BP*-}n\text{-BH} \quad (2)$$

$${}^3\text{BP*-}n\text{-BH} \xrightarrow{\text{HA}} {}^3[\text{BPH}^\bullet\text{-}n\text{-BPH}^\bullet] \quad (3)$$

$${}^3[\text{BPH}^\bullet\text{-}n\text{-BPH}^\bullet] \xrightarrow{\text{ISC}} {}^1[\text{BPH}^\bullet\text{-}n\text{-BPH}^\bullet] \quad (4)$$

$${}^1[\text{BPH}^\bullet\text{-}n\text{-BPH}^\bullet] \rightarrow \text{recombination products} \quad (5)$$

$${}^3[\text{BPH}^\bullet\text{-}n\text{-BPH}^\bullet] \rightarrow \text{monoradicals} \quad (6)$$

$${}^3[\text{BPH}^\bullet\text{-}n\text{-BPH}^\bullet] \xrightarrow{\text{SO-induced ISC}} \text{products} \quad (7)$$

The triplet biradical ^{3}[BPH$^\bullet$-*n*-BPH$^\bullet$] undergoes intersystem crossing (ISC) to the singlet biradical ^{1}[BPH$^\bullet$-*n*-BPH$^\bullet$] (eq 4)

TABLE 1: Lifetimes (μs) of ^{3}BP*-*n*-BH[a]

^{12}C-BP-12-BH-^{12}C	3.3
^{13}C-BP-12-BH-^{12}C	3.5
^{12}C-BP-12-BH-^{13}C	3.5
^{13}C-BP-12-BH-^{13}C	3.7
^{2}H-BP-12-BH-^{1}H	4.3
^{1}H-BP-12-BH-^{2}H	4.4
^{2}H-BP-12-BH-^{2}H	4.4
^{12}C-BP-10-BH-^{12}C	3.5
^{13}C-BP-10-BH-^{12}C	4.1
^{13}C-BP-10-BH-^{13}C	4.3
^{12}C-BP-8-BH-^{12}C	3.0
^{13}C-BP-8-BH-^{12}C	3.4
^{13}C-BP-8-BH-^{13}C	4.0

[a] Experimental error is about 10%.

and is thought to result in a recombination reaction (eq 5). The triplet biradical is considered to react with impurities contaminated in benzene followed by generation of the corresponding monoradicals such as BPH•-*n*-BPHH (eq 6). The triplet biradical disappears partly *via* spin−orbit (SO)-induced ISC to the ground state (eq 7). The external magnetic field affects the ISC (eq 4) to change the triplet biradical lifetime.

3.2. Lifetimes of ^{3}BP*-12-BH. The lifetimes of ^{3}BP*-12-BH and its isotope-substituted compounds were calculated from the decay profiles at 620 nm, since those observed at 600−650 nm were independent of the magnetic field. The results are summarized in Table 1. When ^{13}C and ^{2}H atoms were substituted at the benzylic position and in the phenyl rings, respectively, the lifetime slightly increased with increasing extent of ^{13}C and ^{2}H substitutions. For ^{13}C-BP-12-BH-^{13}C and ^2H-BP-12-BH-^2H, the increments in lifetimes were calculated to be 12 and 33%, respectively, compared with that of naturally abundant ^{12}C-BP-12-BH-^{12}C. The increment in the ^{2}H substitution was relatively large.

3.3. MFEs and MIEs on Biradical Lifetimes and Dependence of Biradical Lifetimes on Methylene Chain Length. Biradical lifetimes in the presence of a magnetic field were estimated from measurement at 350 nm where the absorbance due to BPH• was dominant. Because the absorption due to ^{3}BP*-12-BH overlapped the absorptions due to BPH•-12-BPH• (eqs 3 and 4), mono BPH• radical (eq 6), and reaction products (eqs 5 and 7), the decay profiles at 350 nm were analyzed by the following equation:

$$A(t) = A(1)\exp(-t/\tau_{BR}) + A(2)\exp(-t/\tau_T) + A(3) \quad (8)$$

where $A(t)$ is absorbance at time t, τ_{BR} and τ_T are lifetimes of the biradical and ^{3}BP*, $A(1)$ and $A(2)$ are their pre-exponential factors, and $A(3)$ is the absorbance due to reaction products and mono BPH•, since the mono BPH• does not practically decay because of its low concentration, as shown in an inset in Figure 1b. The values of τ_T were taken from Table 1 and were fixed throughout the analyses of the decay profiles at 350 nm.

The results for BPH•-12-BPH• and related biradicals are summarized in Figures 2 and 3 and Table 2. The biradical lifetimes at 0 T were not obtained, as discussed in section 3.1. In the case of BPH•-12-BPH•, the lifetime steeply increased up to *ca*. 8 μs at 3 T as the magnetic field increased and then it appeared to slightly dwindle to 7.2 μs at 13 T. The lifetime at 3 T increased up to *ca*. 140% of that at 0.15 T, and the lifetime at 13 T decreased to *ca*. 90% of the maximum lifetime (*ca*. 8 μs). This effect, that is, a reversal of the MFE on the lifetime, is thought to be characteristic only of high magnetic fields above 2 T.[5c−d,8,9,10,12,19−22] A similar MFE was also observed in other biradicals of $n = 8$ and 10.

The MIEs on the magnetic field dependences (MFDs) of biradical lifetimes in ^{13}C and ^{2}H substitutions are also demonstrated in Figures 2 and 3 and Table 2. In the ^{13}C substitution, the change in lifetimes was remarkable around 0.5 T. *The large MIE was observed only below ca. 3 T, where the biradical lifetime was increasing, and the lifetime difference among the*

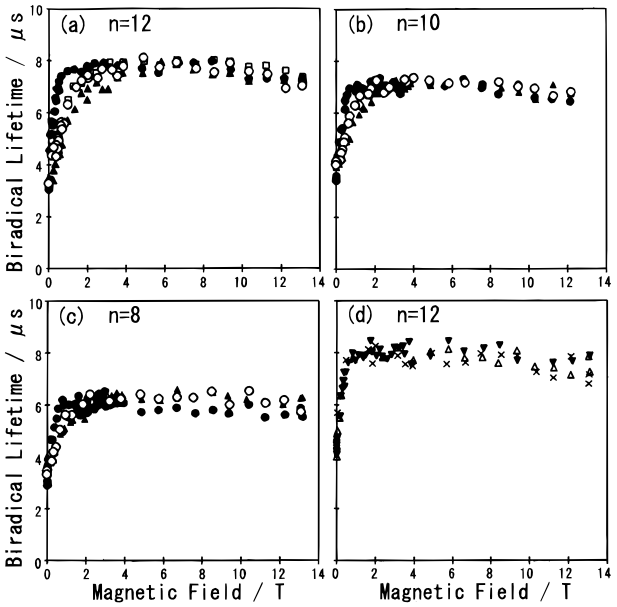

Figure 2. MFD of τ_{BR} of BPH•-*n*-BPH• biradicals, where the parent molecules are the following: (●) ^{12}C-BP-*n*-^{12}C-BH; (○) ^{13}C-BP-*n*-^{12}C-BH; (□) ^{12}C-BP-*n*-^{13}C-BH; (▲) ^{13}C-BP-*n*-^{13}C-BH; (▼) ^{1}H-BP-12-^{2}H-BH; (△) ^{2}H-BP-12-^{1}H-BH; (×) ^{2}H-BP-12-^{2}H-BH; (a) $n = 12$; (b) $n = 10$; (c) $n = 8$; (d) $n = 12$.

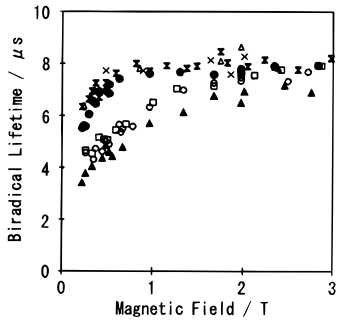

Figure 3. MFD of τ_{BR} of BPH•-12-BPH• biradicals. The range of the abscissa is 0−3 T. The parent molecules are (●) ^{12}C-BP-*n*-^{12}C-BH, (○) ^{13}C-BP-*n*-^{12}C-BH, (□) ^{12}C-BP-*n*-^{13}C-BH, (▲) ^{13}C-BP-*n*-^{13}C-BH, (▼) ^{1}H-BP-12-^{2}H-BH, (△) ^{2}H-BP-12-^{1}H-BH, and (×) ^{2}H-BP-12-^{2}H-BH.

TABLE 2: Lifetimes (μs) of BPH•-*n*-BPH• Biradicals at Magnetic Fields[a]

	magnetic field					
biradical	0.15 T	0.50 T	1.5 T	2.0 T	7.5 T	13 T
^{12}C-BPH•-12-BPH•-^{12}C	5.7	7.0	7.7	7.7	7.9	7.2
^{13}C-BPH•-12-BPH•-^{12}C[b]	4.4	4.9	7.0	7.3	7.7	7.1
^{12}C-BPH•-12-BPH•-^{13}C[c]	4.7	5.1	7.0	7.6	7.9	7.3
^{13}C-BPH•-12-BPH•-^{13}C	3.4	4.6	6.2	7.0	7.7	7.1
^{2}H-BPH•-12-BPH•-^{1}H[d]	5.5	7.1	8.0	8.7	7.8	7.3
^{1}H-BPH•-12-BPH•-^{2}H[e]	5.6	7.5	7.8	7.9	8.2	7.9
^{2}H-BPH•-12-BPH•-^{2}H	6.3	7.7	8.1	8.3	8.0	7.2
^{12}C-BPH•-10-BPH•-^{12}C	4.9	6.7	7.0	7.3	7.0	6.8
^{13}C-BPH•-10-BPH•-^{12}C	4.2	5.3	6.7	6.9	7.1	7.3
^{13}C-BPH•-10-BPH•-^{13}C	4.1	4.9	6.2	6.9	7.1	6.9
^{12}C-BPH•-8-BPH•-^{12}C	4.7	5.7	6.0	6.1	5.7	5.5
^{13}C-BPH•-8-BPH•-^{12}C	3.9	4.7	5.7	6.1	6.3	5.7
^{13}C-BPH•-8-BPH•-^{13}C	3.8	4.6	5.4	6.0	6.8	6.3

[a] Experimental error is about 10%. [b] Obtained from ^{13}C-BP-12-BH-^{12}C. [c] Obtained from ^{12}C-BP-12-BH-^{13}C. [d] Obtained from ^{2}H-BP-12-BH-^{1}H. [e] Obtained from ^{1}H-BP-12-BH-^{2}H.

SCHEME 1

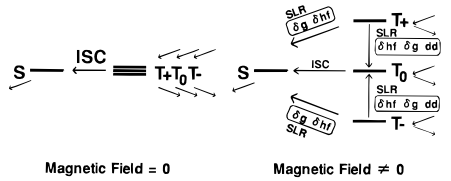

isotope-substituted biradicals was not detected above 4 T within experimental accuracy. The steep increase in lifetimes was conspicuous when carbon atoms at benzylic positions of both BP and BH in BP-*n*-BH were in natural abundance (^{12}*C*-BP-*n*-BH-^{12}*C*). For example, the lifetimes at 0.5 T were 7.0 μs (^{12}*C*-BPH$^{\bullet}$-12-BPH$^{\bullet}$-^{12}*C*), 4.9 μs (^{13}*C*-BPH$^{\bullet}$-12-BPH$^{\bullet}$-^{12}*C*), 5.1 μs (^{12}*C*-BPH$^{\bullet}$-12-BPH$^{\bullet}$-^{13}*C*), and 4.6 μs (^{13}*C*-BPH$^{\bullet}$-12-BPH$^{\bullet}$-^{13}C), respectively. Here, ^{13}*C*-BPH$^{\bullet}$-12-BPH$^{\bullet}$-^{12}*C* and ^{12}*C*-BPH$^{\bullet}$-12-BPH$^{\bullet}$-^{13}*C* were generated from ^{13}*C*-BP-12-BH-^{12}*C* and ^{12}*C*-BP-12-BH-^{13}*C*, respectively. Furthermore, the biradicals (^{13}*C*-BPH$^{\bullet}$-*n*-BPH$^{\bullet}$-^{12}*C*, ^{12}*C*-BPH$^{\bullet}$-*n*-BPH$^{\bullet}$-^{13}*C*, and ^{13}*C*-BPH$^{\bullet}$-*n*-BPH$^{\bullet}$-^{13}*C*) derived from ^{13}C-substituted BP-*n*-BH compounds tended to require a higher magnetic field intensity to reach the maximum lifetime along with the extent of the ^{13}C substitution. The magnetic fields at which the maximum lifetimes were obtained were about 2.5 T (^{12}*C*-BPH$^{\bullet}$-12-BPH$^{\bullet}$-^{12}*C*), 4.5 T (^{13}*C*-BPH$^{\bullet}$-12-BPH$^{\bullet}$-^{12}*C*), 4.5 T (^{12}*C*-BPH$^{\bullet}$-12-BPH$^{\bullet}$-^{13}*C*), and 6.5 T (^{13}*C*-BPH$^{\bullet}$-12-BPH$^{\bullet}$-^{13}*C*), respectively. In the ^{2}H substitution in the phenyl rings, on the other hand, there was no detectable MIE on the MFD of lifetimes, as shown in Figure 3.

In magnetic fields above 4 T there seemed to be a slightly monotonic decrease and no MIE on the MFD of biradical lifetimes in ^{13}C and ^{2}H substitutions. For example, all the biradical lifetimes in $n = 12$ were about 7.2 μs at 13 T regardless of the isotope substitutions.

Furthermore, dependence of the lifetimes on the chain length (n) was slightly detected in the magnetic fields. Figure 2 also showed a tendency for the biradical lifetimes to become longer as n is increased: $\tau_{BR} = 7.2$, 6.8, and 5.5 μs for $n = 12$, 10, and 8 of the naturally abundant biradicals at 13 T, respectively.

4. Discussion

4.1. Isotope Effects on ^{3}BP*-*n*-BH Lifetimes. The lifetime of ^{3}BP*-*n*-BH was affected by isotope substitution, as shown in Table 1. The lifetime increase in BP-12-BH by ^{13}C substitution was 12%, whereas the increase by ^{2}H substitution was 33%. In cases of ^{2}*H*-BPH$^{\bullet}$-12-BPH$^{\bullet}$-^{1}*H*, ^{1}*H*-BPH$^{\bullet}$-12-BPH$^{\bullet}$-^{2}*H*, and ^{2}*H*-BPH$^{\bullet}$-12-BPH$^{\bullet}$-^{2}*H*, the nonradiative decay from ^{3}BP* may be reduced by the perdeuterated BP, as known from the deuterium isotope effect.[23] The lifetime change induced by the double ^{13}C substitution increased from 12 to 30% with decreasing n from 12 to 8. At the moment we have no possible explanation for this n dependence.

4.2. Mechanism of MFEs on Biradical Lifetimes. Scheme 1 shows the energy diagrams of a biradical in the absence and presence of a magnetic field when the exchange interaction is negligibly small. In the absence of a magnetic field, the triplet biradical is found to disappear *via* eqs 4 and 5. The rate-determining step in those processes is considered to be the HA (eq 3) of ^{3}BP* having a 3.3 μs decay time in BP-12-BH. In general, in the presence of a magnetic field, T_0-S ISC is controlled by both isotropic hyperfine coupling (HFC) and Δg mechanisms in which Δg is a difference of the g values of the two-component radicals. The ISCs of $T_{\pm} \rightarrow S$ are quenched because of the Zeeman splitting of these sublevels from the T_0 sublevel. However, these two mechanisms seem to be irrelevant to the results obtained here because of the following reasons. (i) Although the isotropic HFC mechanism should be significant below *ca.* 0.1 T, the MFE in magnetic fields higher than 0.2 T is discussed in this work. (ii) The Δg mechanism is inadequate to explain the decrease in lifetimes in high magnetic fields because the Δg value is exactly zero in these biradicals because the component radicals are identical. The mechanism of $S-T_-$ mixing was not seen in these biradicals.

In contrast, the SLR mechanism becomes significant in magnetic fields above 0.1 T. Because the biradical lifetimes in magnetic fields were longer than that (3.3 μs) of ^{3}BP*, the rate-determining steps are considered to be $T_{\pm} \rightarrow T_0$ and $T_{\pm} \rightarrow S$ transitions, as shown in Scheme 1. In the SLR of biradicals, the $T_{\pm} \rightarrow T_0$ and $T_{\pm} \rightarrow S$ transitions are usually modulated by three interactions: the *anisotropic* hyperfine (δhf) and *anisotropic* Zeeman (δg) interactions, and the inter-radical electron dipole−dipole (dd) interaction. These three interactions may play an important role in the MFD in high magnetic fields. In the case where the initially populated state of the biradical is a triplet, the biradical populated in the S and T_0 states cannot go on the substates $T_{\pm}$ because of the very fast $T_0 \rightarrow S \rightarrow P$ process. The biradical deactivation in magnetic fields can be assumed to be controlled mainly by the $T_{\pm} \rightarrow T_0$ and $T_{\pm} \rightarrow S$ pathways.

Therefore, the observed decay rate constant k_{BR} of a biradical composed of radicals 1 and 2 is expressed by[4c]

$$k_{BR} = 1/\tau_{BR} = {}^{1}/_{2}\{W(1{:}\delta\mathrm{hf},\delta g) + W(2{:}\delta\mathrm{hf},\delta g)\} + W(\mathrm{dd}) + k_T \quad (9)$$

where $W(1{:}\delta\mathrm{hf},\delta g)$ and $W(2{:}\delta\mathrm{hf},\delta g)$ are the SLR rate constants governed by the δhf and δg interactions in each component radical and W(dd) is the SLR rate constant determined by the dd interaction in the biradical. The term k_T is the rate constant for the disappearance directly from the triplet biradical sublevels that includes the magnetic-field-independent SO-induced ISC (eq 7) and other magnetic-field-independent processes (eq 6). Because the present biradical is composed of two equivalent BPH$^{\bullet}$s, eq 9 can be simplified as

$$k_{BR} = 1/\tau_{BR} = {}^{1}/_{2}\{2W(\mathrm{BPH}^{\bullet}{:}\delta\mathrm{hf},\delta g)\} + W(\mathrm{dd}) + k_T \quad (10)$$

By use of the explicit expression for δhf, δg, and dd interactions modulating the SLR, eq 10 is rewritten as a function of the external magnetic field (B_0):

$$k_{BR} = 1/\tau_{BR} = {}^{1}/_{2}[2\{({}^{1}/_{5})(\beta/\hbar)^2(g{:}g){B_0}^2 + \gamma^2{H_{loc}}^2\}\tau_c/(1 + \gamma^2{B_0}^2{\tau_c}^2)] + \gamma^2{H_{dd}}^2\tau_c'/(1 + \gamma^2{B_0}^2\tau_c'^2) + k_T \quad (11)$$

where γ is the magnetogyric ratio of the electron on BPH$^{\bullet}$ and is assumed to be equal to that of a free electron. The parameters τ_c and τ_c' are rotational correlation times of tumbling Brownian motion for anisotropic interactions (δhf and δg) of BPH$^{\bullet}$ and for the dd interaction between the two BPH$^{\bullet}$s, respectively. The parameter ($g{:}g$) is an inner product of the anisotropic **g** tensor. The parameter H_{loc} is a locally fluctuating magnetic field due to the δhf interaction, which is exactly expressed by a product of the quantum number of the nuclear spin, the isotropic HFC constant, and the spin density (see Appendix). The value ${H_{loc}}^2$ for biradicals is defined as $H_{loc}(1)^2 + H_{loc}(2)^2$ using each value for radicals 1 and 2. The value H_{dd} is a locally fluctuating magnetic field due to the dd interaction of the biradical. According to the theory for the SLR,[24,25] the SLR rate due to the δhf and dd interactions decreases as the external magnetic field increases, whereas the rate due to the δg interaction increases. Therefore, the MFD shown in Figure 2 is classified

TABLE 3: Calculated Local Magnetic Fields (H_{loc}) by the δhf Interaction

radicals and biradicals	$H_{loc}/10^{-4}$ T	$H_{loc}^2/10^{-8}$ T^2 [a]
^{12}C-BPH$^\bullet$	1.76	3.10
^{13}C-BPH$^\bullet$	9.43	88.9
^{2}H-BPH$^\bullet$	0.746	0.556
^{12}C-BPH$^\bullet$-*n*-BPH$^\bullet$-^{12}C	2.49	6.20
^{13}C-BPH$^\bullet$-*n*-BPH$^\bullet$-^{12}C	9.59	92.0
^{13}C-BPH$^\bullet$-*n*-BPH$^\bullet$-^{13}C	13.3	178
^{2}H-BPH$^\bullet$-12-BPH$^\bullet$-^{1}H	1.91	3.66
^{2}H-BPH$^\bullet$-12-BPH$^\bullet$-^{2}H	1.06	1.11

[a] The values for biradicals were evaluated by $H_{loc}(1)^2 + H_{loc}(2)^2$ with H_{loc}(1 and 2) for the component radicals 1 and 2.

into two magnetic field regions of 0.1−3 T and 4−13 T. In the former region the biradical lifetime increases as the external magnetic field increases, whereas in the latter the lifetime decreases.

4.3. MFEs and MIEs in 0.1−3 T. As already described, because biradical lifetimes increased in 0.1−3 T, the δhf and dd interactions should be discussed as mechanisms for the MFE. The biradical lifetimes in ^{13}C-BPH$^\bullet$-*n*-BPH$^\bullet$-^{13}C showed a large decrease compared with those in ^{12}C-BPH$^\bullet$-*n*-BPH$^\bullet$-^{12}C, as shown in Figures 2 and 3 and Table 2. The large MIE due to ^{13}C substitution should be very important because such an MIE above 2 T is unprecedented, though there are many reports about MIEs below 0.1 T.[4b] The result of the MIE presents the best evidence for the type of magnetic interaction in the biradical that is responsible for the lifetime change in high magnetic fields. The appearance of the MIE means that the dominant biradical deactivation in magnetic fields is the SLR, which is mainly due to the δhf interaction, not to the dd interaction. If the dd interaction is of primary importance to the increase in lifetimes, no such MIE should appear because the most effective dd interaction is due to two electron spins on the component radicals, not nuclear spins.

Because no decrease in lifetimes due to the δg interaction is observed in 0.1−3 T as shown in Figures 2 and 3, the δg interaction can be excluded from eq 11. Hence, eq 11 can be simplified as

$$k_{BR} = 1/\tau_{BR} = {}^1/_2[\gamma^2(2H_{loc}{}^2)\tau_c/(1+\gamma^2B_0{}^2\tau_c{}^2)] + \gamma^2H_{dd}{}^2\tau_c'/(1+\gamma^2B_0{}^2\tau_c'{}^2) + k_T \quad (12)$$

The MIE on the biradical lifetimes is associated with H_{loc}, since H_{loc} is the only parameter in eq 12 that is dependent on nuclear spins. The values $H_{loc}{}^2$ for isotope-substituted biradicals were theoretically estimated with electron spin density and isotropic HFC constants according to a procedure reported in a previous paper.[26] The results are listed in Table 3. For biradicals composed of ^{12}C- and ^{13}C-BPH$^\bullet$s, the theoretical values qualitatively explain the experimental data of MIEs on lifetimes shown in Figures 2 and 3 and Table 2. That is, a large value of $H_{loc}{}^2$ means a small biradical lifetime. There is a large difference in the theoretical $H_{loc}{}^2$ between ^{12}C-BPH$^\bullet$-12-BPH$^\bullet$-^{12}C and ^{13}C-BPH$^\bullet$-12-BPH$^\bullet$-^{13}C, which corresponds to that in the lifetimes (7.0 and 4.6 μs at 0.5 T; see Table 2) between them. On the other hand, although the theoretical $H_{loc}{}^2$ for ^{12}C-BPH$^\bullet$-12-BPH$^\bullet$-^{12}C is about 6 times larger than that for ^{2}H-BPH$^\bullet$-12-BPH$^\bullet$-^{2}H, there is no difference in lifetimes between them as shown in Figure 3. This implies that another mechanism that is independent of nuclear spins is operative in them. Because the lifetime increases in 0.1−3 T, the dominant mechanism might be the dd interaction rather than the δhf interaction. This is supported by the fact that the dd interaction is independent of nuclear spins. It may be stated that the SLR in ^{13}C-BPH$^\bullet$-12-BPH$^\bullet$-^{13}C and ^{13}C-BPH$^\bullet$-12-BPH$^\bullet$-^{12}C is controlled by the δhf interaction, whereas that in ^{12}C-BPH$^\bullet$-12-BPH$^\bullet$-^{12}C, ^{2}H-BPH$^\bullet$-12-BPH$^\bullet$-^{1}H, and ^{2}H-BPH$^\bullet$-12-BPH$^\bullet$-^{2}H is modulated mainly by the dd interaction. Therefore, several parameters in the δhf and dd interactions in eq 12 are evaluated from the MFDs of ^{13}C-BPH$^\bullet$-12-BPH$^\bullet$-^{13}C and ^{2}H-BPH$^\bullet$-12-BPH$^\bullet$-^{2}H, respectively, compared with that of ^{12}C-BPH$^\bullet$-12-BPH$^\bullet$-^{12}C.

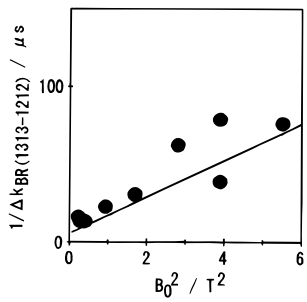

Figure 4. Plots of $1/\Delta k_{BR(1313\text{-}1212)}$ versus $B_0{}^2$. The value of $1/\Delta k_{BR(1313\text{-}1212)}$ was obtained from eq 14.

4.3.1. Evaluation of Parameters for the δhf Interaction from Comparison of ^{13}C-BPH$^\bullet$-12-BPH$^\bullet$-^{13}C with ^{12}C-BPH$^\bullet$-12-BPH$^\bullet$-^{12}C. By use of the MFD data of ^{13}C-BPH$^\bullet$-12-BPH$^\bullet$-^{13}C and ^{12}C-BPH$^\bullet$-12-BPH$^\bullet$-^{12}C, τ_c and the difference ($\Delta H_{loc}{}^2$) in $H_{loc}{}^2$ between them can be experimentally obtained. Let us now consider the difference ($\Delta k_{BR(1313\text{-}1212)}$) in k_{BR} between ^{13}C-BPH$^\bullet$-12-BPH$^\bullet$-^{13}C and ^{12}C-BPH$^\bullet$-12-BPH$^\bullet$-^{12}C. Because the only term in eq 12, which is dependent on the nuclear spin of ^{13}C is $H_{loc}{}^2$, the terms for the dd interaction and k_T are canceled, and then $\Delta k_{BR(1313\text{-}1212)}$ is derived from eq 12 as

$$\Delta k_{BR(1313\text{-}1212)} = k_{BR(1313)} - k_{BR(1212)} = {}^1/_2[\gamma^2\{2H_{loc}{}^2{}_{(13)} - 2H_{loc}{}^2{}_{(12)}\}\tau_c/(1+\gamma^2B_0{}^2\tau_c{}^2)] = {}^1/_2[\gamma^2(2\Delta H_{loc}{}^2{}_{(13\text{-}12)})\tau_c/(1+\gamma^2B_0{}^2\tau_c{}^2)] \quad (13)$$

where the subscripts, (1313), (1212), (13) and (12) signify ^{13}C-BPH$^\bullet$-12-BPH$^\bullet$-^{13}C, ^{12}C-BPH$^\bullet$-12-BPH$^\bullet$-^{12}C, ^{13}C-BPH$^\bullet$, and ^{12}C-BPH$^\bullet$, respectively. The reciprocal of eq 13 is

$$1/\Delta k_{BR(1313\text{-}1212)} = 2[1/\{\gamma^2(2\Delta H_{loc}{}^2{}_{(13\text{-}12)})\tau_c\} + \tau_cB_0{}^2/(2\Delta H_{loc}{}^2{}_{(13\text{-}12)})] \quad (14)$$

Therefore, when the data of $1/\Delta k_{BR(1313\text{-}1212)}$ are redrawn versus $B_0{}^2$, τ_c and $\Delta H_{loc}{}^2$ for the biradical are obtained from the intercept and slope.

Figure 4 shows the plot of $1/\Delta k_{BR(1313\text{-}1212)}$ versus $B_0{}^2$. The values of τ_c and $\Delta H_{loc}{}^2{}_{(13\text{-}12)}$ were calculated to be 8.1 ps and 69×10^{-8} T^2, respectively. From the theoretical estimation of the two biradicals shown in Table 3, the $\Delta H_{loc}{}^2{}_{(13\text{-}12)}$ is estimated to be 85.8×10^{-8} T^2. The agreement between the theoretical value and experimental one rationalizes the application of the values in Table 3 to the estimation of $H_{loc(13)}$. The experimentally obtained value $H_{loc(13)}$ was determined to be 8.1×10^{-4} T from the relationship $H_{loc}{}^2{}_{(13)} = H_{loc}{}^2{}_{(12)} + \Delta H_{loc}{}^2{}_{(13\text{-}12)}$ based on the theoretical value ($H_{loc(12)} = 1.76 \times 10^{-4}$ T) in Table 3. Similarly, the values of τ_c and $H_{loc(13)}$ were obtained to be 7.9 ps and 6.1×10^{-4} T from the data of ^{13}C-BPH$^\bullet$-12-BPH$^\bullet$-^{12}C and ^{12}C-BPH$^\bullet$-12-BPH$^\bullet$-^{12}C. The calculated $H_{loc(13)}$ values listed in Table 4 are close to the theoretical one (9.43×10^{-4} T) in Table 3 and the experimental one (17×10^{-4} to 27×10^{-4} T)

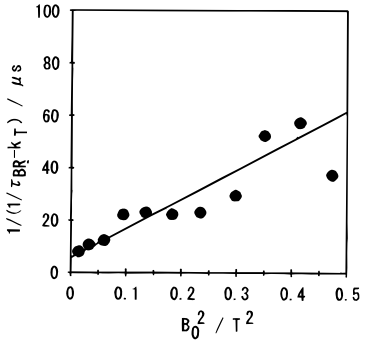

Figure 5. Plots of $1/(1/\tau_{BR} - k_T)$ versus B_0^2. The value of $1/(1/\tau_{BR} - k_T)$ was obtained from eq 15.

TABLE 4: Parameters Obtained from the Analyses of the MFDs of BPH•-12-BPH• Biradicals

$H_{loc(13)}/10^{-4}$ T	8.1[a]	6.1[b]
τ_c/ps	8.1[a]	7.9[b]

[a] Obtained from ^{13}C-BPH•-12-BPH•-^{13}C and ^{12}C-BPH•-12-BPH•-^{12}C. [b] Obtained from ^{13}C-BPH•-12-BPH•-^{12}C and ^{12}C-BPH•-12-BPH•-^{12}C.

reported in ^{13}C-BPH•, which was generated from ^{13}C-substituted benzophenone.[27] We have reported $\tau_c = 10$ ps for a biradical derived from BP−CO_2−$(CH_2)_{12}$−O−DPM and $\tau_c = 12$ ps for a biradical derived from BP−CO_2−$(CH_2)_{12}$−O−PET.[10] The value ($\tau_c = 8.1$ ps) obtained in this work is comparable to those reported within experimental accuracy.

A similar estimate of τ_c and H_{loc} for ^2H-BPH• could not be carried out because there is no significant difference between the data of ^2H-BPH•-12-BPH•-^2H and ^{12}C-BPH•-12-BPH•-^{12}C, as previously mentioned.

4.3.2. Dominant Contribution of the dd Interaction to the MFDs of Naturally Abundant and Deuterated Biradicals. If the biradical SLR at 0.1−3 T is predominantly controlled by the δhf interaction, the difference in the MFD data should be observed, since the theoretical H_{loc}^2 value (6.20×10^{-8} T^2) for ^{12}C-BPH•-12-BPH•-^{12}C is 6 times larger than that (1.11×10^{-8} T^2) for ^2H-BPH•-12-BPH•-^2H (see Table 3). There is, however, no significant difference between the MFD data of ^2H†-BPH•-12-BPH•-^2H and ^{12}C-BPH•-12-BPH•-^{12}C, as shown in Figure 3. This fact implies that the dominant interaction responsible for the MFDs of ^2H-BPH•-12-BPH•-^2H, ^2H-BPH•-12-BPH•-^1H, ^1H-BPH•-12-BPH•-^2H, and ^{12}C-BPH•-12-BPH•-^{12}C is the dd interaction of the biradicals. Therefore, an evaluation of the H_{dd} parameter for the dd interaction was carried out with their MFD data. By neglecting the δhf term from eq 12, the equation for the deuterated and naturally abundant biradicals is obtained as

$$1/(k_{BR} - k_T) = 1/(1/\tau_{BR} - k_T) = 1/(\gamma^2 H_{dd}^2 \tau_c') + \tau_c' B_0^2/H_{dd}^2 \quad (15)$$

Figure 5 shows a plot of eq 15 for ^2H-BPH•-12-BPH•-^2H where k_T is assumed to be 14×10^4 s^{-1}. The H_{dd} and τ_c' were obtained to be $(4.7 \pm 1.3) \times 10^{-4}$ T and 25 ± 13 ps, respectively, from the intercept and slope in Figure 5. The similar values were obtained in other biradicals, as summarized in Table 5.

Figure 6 depicts the MFDs of the inverses of the SLR rates due to the dd and δhf interactions in ^{12}C-BPH•-12-BPH•-^{12}C ($H_{loc} = 2.49 \times 10^{-4}$ T, $\tau_c = 8.1$ ps, $H_{dd} = 4.7 \times 10^{-4}$ T, and $\tau_c' = 25$ ps) (Figure 6a) and ^{13}C-BPH•-12-BPH•-^{13}C ($H_{loc} = 13.3 \times 10^{-4}$ T, $\tau_c = 8.1$ ps, $H_{dd} = 4.7 \times 10^{-4}$ T, and $\tau_c' = 25$ ps) (Figure 6b). As expected, the contribution of the dd interaction is remarkable in the former lifetime, whereas the δhf interaction chiefly determines the biradical lifetime in the latter. Very recently, we have estimated $H_{dd} = 9.05 \times 10^{-4}$ and 14.3×10^{-4} T for triplet biradicals that resulted from the photoinduced HA in BP−CO_2−$(CH_2)_{12}$−O−DPM and BP−CO_2−$(CH_2)_{12}$−O−PET, respectively, assuming that the two rotational correlation times for the δhf and dd interactions are the same.[10] The H_{dd} values in Table 5 obtained in this work are comparable to those reported within experimental accuracy. In a previous paper,[26] MFEs (<0.6 T) on the lifetimes of triplet biradicals generated from the photolysis of xanthone−CO_2−$(CH_2)_n$−OCO−xanthene (n = 10, 12, 16, and 20) ($H_{loc} = 6.1 \times 10^{-4}$ T) and BP−O−$(CH_2)_n$−O−diphenylamine (n = 10, 12, 14, and 18) ($H_{loc} = 10.1 \times 10^{-4}$ T) were assumed to be caused by the δhf interaction. From the present results on the MIEs, the MFEs of the former and latter biradicals may be due to the dd interaction and to the δhf−dd hybrid interaction, respectively, since the former and latter biradical H_{loc} values are close to those of ^{12}C-BPH•-12-BPH•-^{12}C ($H_{loc} = 2.49 \times 10^{-4}$ T) and ^{13}C-BPH•-12-BPH•-^{13}C ($H_{loc} = 13.3 \times 10^{-4}$ T), respectively.

TABLE 5: Parameters for the dd Interaction Obtained from the Analyses of the MFDs of Deuterated and Naturally Abundant BPH•-12-BPH• Biradicals

biradical	$H_{dd}/10^{-4}$ T	τ_c'/ps	R/nm	$k_T/10^4$ s^{-1}
^2H-BPH•-12-BPH•-^2H	4.7 ± 1.3	25 ± 13	1.3 ± 0.12	14
^2H-BPH•-12-BPH•-^1H[a]	4.8 ± 1.3	28 ± 15	1.3 ± 0.12	14
^1H-BPH•-12-BPH•-^2H[b]	3.5 ± 1.9	25 ± 27	1.4 ± 0.26	14
^{12}C-BPH•-n-BPH•-^{12}C	4.4 ± 1.6	26 ± 20	1.3 ± 0.16	14

[a] Obtained from ^2H-BP-12-BH-^1H. [b] Obtained from ^1H-BP-12-BH-^2H.

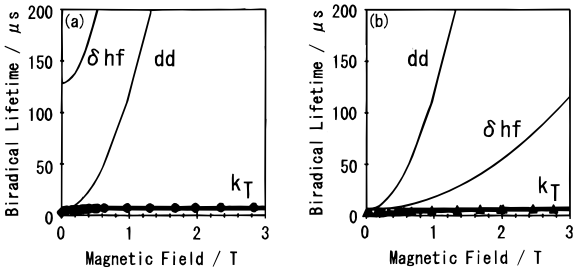

Figure 6. Experimentally obtained (●, ▲) and calculated (−) MFDs by the respective contributions of δhf, dd, and k_T in (a) ^{12}C-BPH•-12-BPH•-^{12}C and (b) ^{13}C-BPH•-12-BPH•-^{13}C. The bold lines show the total contribution by those three terms. The parameters used in eq 12 are $H_{loc(12)} = 1.76 \times 10^{-4}$ T, $H_{loc(13)} = 8.1 \times 10^{-4}$ T, $\tau_c = 8.1$ ps, $H_{dd} = 4.7 \times 10^{-4}$ T, and $k_T = 14 \times 10^4$ s^{-1}.

TABLE 6: Inter-radical Distance Simulated by the MC/SD Method of the MacroModel

	$n = 8$	$n = 10$	$n = 12$
R/nm	1.7	1.8	1.9

The mean distance of two radical centers is obtained from H_{dd} with the relation $H_{dd}^2 = (^3/_{10})\hbar^2\gamma^2R^{-6}$ where R is the distance between two electron spins.[25] The distance R was estimated to be 1.3 ± 0.12 nm for ^2H-BPH•-12-BPH•-^2H, as summarized in Table 5. The values in this work are also close to our previous results obtained in the biradicals generated from BP−CO_2−$(CH_2)_{12}$−O−DPM (R = 1.04 nm) and BP−CO_2−$(CH_2)_{12}$−O−PET (R = 0.89 nm).[10] Furthermore, the molecular dynamics simulation by the MC/SD method provided a similar R value (1.9 nm) for n = 12, as listed in Table 6. The consistency in H_{dd} and R with values so far reported and simulated suggests that the SLRs in the deuterated and naturally abundant biradicals are controlled by the dd interaction of the biradicals. If the Stokes−Einstein−Debye (SED) equation is used for the τ_c' calculation, the distance R could be obtained also from the calculated τ_c'. However, the τ_c' calculation with

the SED equation was not carried out at the present stage, since there are many controversies in using the SED equation for the τ_c' estimation (for example, lots of τ_c' values experimentally obtained are smaller than that calculated with the SED equation).[28]

4.4. MFEs and MIEs in 4−13 T. In magnetic fields above 4 T, the MIE disappeared as shown in Figure 2. This indicates that the δhf interaction does not play an important role in this magnetic field region. A slight decrease in lifetimes was also observed in the MFD curves. The biradical lifetimes of ^{12}C-BPH$^{\bullet}$-12-BPH$^{\bullet}$-^{12}C in Table 2 show the decrease from 7.7 μs at 2.0 T to 7.2 μs at 13 T. The numerator in the first term on the right-hand side of eq 11 consists of two terms $(({}^1/_5)(\beta/\hbar)^2(g{:}g)B_0{}^2$ and $\gamma^2H_{loc}{}^2$ for the δg and δhf interactions, respectively). The δg term has the variable B_0, whereas the δhf one does not. Since the denominator $(1 + \gamma^2B_0{}^2\tau_c{}^2)$ is common for both terms, the δg interaction accelerates the SLR with increasing magnetic fields (B_0) whereas the δhf interaction decelerates the SLR. The slight decrease in the high magnetic fields, therefore, implies a contribution of the δg interaction to the biradical SLR. Since the δg interaction is independent of nuclear spins, no detectable MIE above 4 T is realistic. Tanimoto's,[5c,5d,8b−d,9,12b] Nakagaki's,[10,12a] and Hayashi's groups[19,21c,22b] reported the great importance of the δg interaction to the SLR in many biradical and radical pairs and evaluated the anisotropic g values and rotational correlation times. However, in the case of the present biradicals, the decrease in lifetimes is too small to evaluate those parameters. For that purpose, the higher magnetic field intensity may be necessary.

4.5. Dependence of Biradical Lifetimes on Methylene Chain Length. The biradical lifetimes at 13 T become longer as the chain length n increases: $\tau_{BR} = 7.2$, 6.8, and 5.5 μs for $n = 12$, 10, and 8, respectively, of ^{12}C-BPH$^{\bullet}$-n-BPH$^{\bullet}$-^{12}C (see Table 2). This n dependence is observed for magnetic fields up to 14 T. The interactions showing the n dependence are the dd interaction in the SLR in eq 9 and the SO-induced ISC in eq 7. According to eq 12 and the relation $H_{dd}{}^2 = ({}^3/_{10})\hbar^2\gamma^2R^{-6}$ for the dd interaction, the dd interaction depends on the distance (R) between the component radicals and lengthens the biradical lifetime with an increase in R. The results for R ($R = 1.7$, 1.8, and 1.9 nm for $n = 8$, 10, and 12, respectively) obtained by the MC/SD molecular dynamics simulation predict a trend toward longer lifetimes for $n = 12$ compared with that for $n = 8$ (see Table 6). However, the possibility of the dd interaction may be excluded because its contribution to the SLR in high magnetic fields above 4 T is thought to be too small to explain the n difference in biradical lifetimes. The SO-induced ISC is also dependent on R and independent of the magnetic field intensity. Therefore, the n dependence may be due to the enhanced SO-induced ISC in eq 7.

5. Summary

The MFD of τ_{BR} was found to be controlled by the SLR because of both the δhf interaction of the component BPH$^{\bullet}$ and the dd interaction of the biradical at 0.1−3 T and also because of the δg interaction of the component BPH$^{\bullet}$ beyond 4 T. The large MIE in ^{13}C-BPH$^{\bullet}$-n-BPH$^{\bullet}$-^{13}C suggests the following. (i) The lifetime of ^{13}C-BPH$^{\bullet}$-n-BPH$^{\bullet}$-^{13}C ($H_{loc} \approx 14 \times 10^{-4}$ T) is determined by the δhf interaction, whereas the dd interaction seems to be a minor contribution to the lifetime. (ii) The lifetimes in naturally abundant and deuterated biradicals (^{12}C-BPH$^{\bullet}$-n-BPH$^{\bullet}$-^{12}C, ^2H-BPH$^{\bullet}$-12-BPH$^{\bullet}$-^1H, ^1H-BPH$^{\bullet}$-12-BPH$^{\bullet}$-^2H, and ^2H-BPH$^{\bullet}$-12-BPH$^{\bullet}$-^2H) ($H_{loc} \approx 3 \times 10^{-4}$ T) are mainly determined by the dd interaction. In addition, from the results of quantitative analyses of the large MIE, the fluctuating local magnetic fields and rotational correlation times in the δhf and dd interactions were obtained. The rotational correlation time (25 ps) for the dd interaction was found to be larger than that (8.1 ps) for the δhf interaction.

SCHEME 2

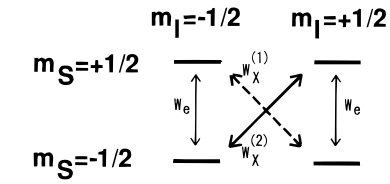

Acknowledgment. This work was financially supported by Grants-in-Aid for Scientific Research (Nos. 04242107, 07NP0101, 07228248, 07740502, 08218243) from the Ministry of Education, Science, Sports and Culture of Japan. We thank Messrs. Ken-ichi Hiruta, Yasunori Miki, Akihiko Hashimoto, and Hiroaki Tanaka for their experimental support.

Appendix

Let us consider the simple case of a hydrogen atom that has single electronic ($m_S = \pm{}^1/_2$) and nuclear ($m_I = \pm{}^1/_2$) spins. Scheme 2 shows the energy diagram at a magnetic field. If the rate constants of the SLRs between $|m_S = +{}^1/_2, m_I = \pm{}^1/_2\rangle$ and $|m_S = -{}^1/_2, m_I = \pm{}^1/_2\rangle$, between $|m_S = +{}^1/_2, m_I = -{}^1/_2\rangle$ and $|m_S = -{}^1/_2, m_I = +{}^1/_2\rangle$, and between $|m_S = +{}^1/_2, m_I = +{}^1/_2\rangle$ and $|m_S = -{}^1/_2, m_I = -{}^1/_2\rangle$ are expressed as W_e, $W_x^{(1)}$, and $W_x^{(2)}$, respectively, the averaged SLR rate $1/T_1$ for a hydrogen atom is

$$ {}^1/_{T_1} = 2(\sum W)/N = 2(2W_e + W_x{}^{(1)} + W_x{}^{(2)})/2 = 2W_e + W_x{}^{(1)} + W_x{}^{(2)} \quad \text{(a1)} $$

where N is the number of nuclear substates (here, $N = 2$). The terms W_e, $W_x^{(1)}$, and $W_x^{(2)}$ for a hydrogen atom are defined as follows. Since $m_I = \pm{}^1/_2$,

$$ W_e = \{({}^1/_8)\gamma^2(t{:}t) \pm ({}^1/_2)(\beta/\hbar)\gamma(t{:}g)B_0 + ({}^1/_2)(\beta/\hbar)^2(g{:}g)B_0{}^2\}({}^1/_5)\tau_c/(1 + \gamma^2B_0{}^2\tau_c{}^2) \quad \text{(a2)} $$

$$ W_x{}^{(1)} = ({}^1/_{12})\gamma^2(t{:}t)({}^1/_5)\tau_c/(1 + \gamma^2B_0{}^2\tau_c{}^2) \quad \text{(a3)} $$

$$ W_x{}^{(2)} = ({}^1/_2)\gamma^2(t{:}t)({}^1/_5)\tau_c/(1 + \gamma^2B_0{}^2\tau_c{}^2) \quad \text{(a4)} $$

where $(t{:}t)$ is an inner product of the δhf tensor. Thus,

$$ {}^1/_{T_1} = \{({}^1/_5)(\beta/\hbar)^2(g{:}g)B_0 + ({}^1/_6)\gamma^2(t{:}t)\}\tau_c/(1 + \gamma^2B_0{}^2\tau_c{}^2) \quad \text{(a5)} $$

Therefore,

$$ H_{loc}{}^2 = ({}^1/_6)(t{:}t) \quad \text{(a6)} $$

The factor ${}^1/_6$ in eq a6 is derived from the quantum number m_I of related nuclei. Since the present biradical (BPH$^{\bullet}$-n-BPH$^{\bullet}$) has three different nuclear spins (^{1}H, ^{2}H, and ^{13}C), the factor is difficult to estimate. Furthermore, because the value $(t{:}t)$ is not known for BPH$^{\bullet}$ and the distribution of spin density should be considered, the fluctuating magnetic field is denoted simply as $H_{loc}{}^2$ in eq 11.

References and Notes

(1) (a) Turro, N. J.; Krautler, B. *Acc. Chem. Res.* **1980**, *13*, 369. (b) Turro, N. J. *Proc. Natl. Acad. Sci. U.S.A.* **1983**, *80*, 609.

(2) (a) Brocklehurst, B. *Int. Rev. Phys. Chem.* **1985**, *4*, 279. (b) Brocklehurst, B.; McLauchlan, K. A. *Int. J. Radiat. Biol.* **1996**, *69*, 3.

(3) (a) Molin, Yu. N. *Spin Polarization and Magnetic Effects in Radical Reactions*; Elsevier: Amsterdam, 1984. (b) Buchachenko, A. L. *Chem. Rev.* **1995**, *95*, 2507.

(4) (a) Schulten, K. *Advances in Solid State Physics*; Viewweg: Braunschweig, 1982; Vol. xxii, p 61. (b) Steiner, U. E.; Ulrich, T. *Chem. Rev.* **1989**, *89*, 51. (c) Steiner, U. E.; Wolff, H.-J. *Photochemistry and Photophylsics*; CRC Press: Boca Raton, FL, 1991; Vol. iv, p 1.

(5) (a) Tanimoto, Y. *Yakugaku Zasshi* **1989**, *109*, 505. (b) Nakagaki, R.; Tanimoto, Y.; Mutai, K. *J. Phys. Org. Chem.* **1993**, *6*, 381. (c) Tanimoto, Y.; Fujiwara, Y. *J. Synth. Org. Chem. Jpn.* **1995**, *53*, 413. (d) Tanimoto, Y. *Hyomen* **1995**, *33*, 282.

(6) (a) Hayashi, H. *Photochemistry and Photophysics*; CRC Press: Boca Raton, FL, 1990; Vol. i, Chapter 2. (b) Hayashi, H.; Sakaguchi, Y. *Lasers in Polymer Science and Technology: Application*; CRC Press: Boca Raton, FL, 1990; Vol. 1, Chapter 1.

(7) (a) Nakamura, H.; Uehata, A.; Motonaga, A.; Ogata, T.; Matsuo, T. *Chem. Lett.* **1987**, 543. (b) Yonemura, H.; Nakamura, H.; Matsuo, T. *Chem. Phys.* **1992**, *162*, 69.

(8) (a) Fujiwara, Y.; Mukai, M.; Tamura, T.; Tanimoto, Y.; Okazaki, M. *Chem. Phys. Lett.* **1993**, *213*, 89. (b) Fujiwara, Y. *Chem. Chem. Ind.* **1995**, *48*, 115. (c) Fujiwara, Y.; Mukai, M.; Tanimoto, Y. *Trans. IEE Jpn.* **1996**, *116A*, 419. (d) Fujiwara, Y.; Aoki, T.; Yoda, K.; Cao, H.; Mukai, M.; Haino, T.; Fukazawa, Y.; Tanimoto, Y.; Yonemura, H.; Matsuo, T.; Okazaki, M. *Chem. Phys. Lett.* **1996**, *259*, 361.

(9) Mukai, M.; Fujiawa, Y.; Tanimoto, Y.; Okazaki, M. *J. Phys. Chem.* **1993**, *97*, 12660.

(10) Nakagaki, R.; Yamaoka, M.; Takahira, O.; Hiruta, K.; Fujiwara, Y.; Tanimoto, Y. *J. Phys. Chem. A* **1997**, *101*, 556.

(11) Nakagaki, R.; Takahira, O.; Hiruta, K. *Chem. Phys. Lett.* **1995**, *233*, 41.

(12) Some preliminary results were published. (a) Takahira, O.; Nakagaki, R.; Fujiwara, Y.; Tanimoto, Y.; Itoh, M. Symposium on Molecular Structure and Molecular Spectroscopy, Tokyo, 1994; Abstract 3bP60. (b) Tanimoto, Y.; Fujiwara, Y.; Mukai, M.; Nakagaki, R.; Okazaki, M. *Abstract of Papers, 3rd International Symposium on Magnetic Field and Spin Effects in Chemistry and Related Phenomena*; Chicago, 1994; pp 52, 84.

(13) Nakagaki, R.; Shimizu, K.; Mutai, K. *Z. Phys. Chem.* **1993**, *182*, 255.

(14) Guarnieri, F.; Still, W. C. *J. Comput. Chem.* **1994**, *15*, 1302.

(15) We are grateful to Professor W. C. Still for providing a copy of this program. Mohamadi, F.; Richards, N. G. J.; Guida, W. C.; Liskamp, R.; Lipton, M.; Caufield, C.; Chang, G.; Hendrickson, T.; Still, W. C. *J. Comput. Chem.* **1990**, *11*, 440.

(16) McDonald, D. Q.; Still, W. C. *J. Am. Chem. Soc.* **1994**, *116*, 11550.

(17) Still, W. C.; Tempczyk, A.; Hawley, R. C.; Hendrickson, T. *J. Am. Chem. Soc.* **1990**, *112*, 6127.

(18) (a) Tanimoto, Y.; Okada, N.; Takamatsu, S.; Itoh, M. *Bull. Chem. Soc. Jpn.* **1990**, *63*, 1342. (b) Buettner, A. V.; Dedinas, J. *J. Phys. Chem.* **1971**, *75*, 187.

(19) Nakamura, Y.; Igarashi, M.; Sakaguchi, Y.; Hayashi, H. *Chem. Phys. Lett.* **1994**, *217*, 387.

(20) Sakaguchi, Y. *Abstract of Papers, 3rd International Symposium on Magnetic Field and Spin Effects in Chemistry and Related Phenomena*; Chicago, 1994; p 113.

(21) (a) Wakasa, M.; Sakaguchi, Y.; Hayashi, H. *Chem. Lett.* **1994**, 49. (b) Wakasa, M.; Igarashi, M.; Sakaguchi, Y.; Hayashi, H. *Chem. Lett.* **1994**, 1941. (c) Igarashi, M.; Meng, Q.-X.; Sakaguchi, Y.; Hayashi, H. *Mol. Phys.* **1995**, *84*, 943.

(22) (a) Wakasa, M.; Hayashi, H. *J. Phys. Chem.* **1995**, *99*, 17074. (b) Wakasa, M.; Hayashi, H.; Mikami, Y.; Takada, T. *J. Phys. Chem.* **1995**, *99*, 133181.

(23) Turro, N. J. *Modern Molecular Photochemistry*; University Science Books: Mill Valley, CA, 1991; Chapter 6.

(24) Abragam, A. *The Principles of Nuclear Magnetism*; Clarendon Press: Oxford, 1961; Chapter 8.

(25) Carrington, A.; MaLachlan, A. D. *Introduction to Magnetic Resonance with Application to Chemistry and Chemical Physics*, Harper and Row: New York, 1967; Chapter 11.

(26) Tanimoto, Y.; Fujiwara, Y.; Takamatsu, S.; Kita, A.; Itoh, M.; Okazaki, M. *J. Phys. Chem.* **1992**, *96*, 9844.

(27) Murai, H.; Jinguji, M.; Obi, K. *J. Phys. Chem.* **1976**, *80*, 429.

(28) (a) Ben-Amotz, D.; Drake, J. M. *J. Chem. Phys.* **1988**, *89*, 1019. (b) Roy, M.; Doraiswamy, S. *J. Chem. Phys.* **1993**, *98*, 3213. (c) Böttcher, C. J. F.; Bordewijk, P. *Theory of Electric Polarization*; Elsevier: Amsterdam, 1978; Vol. 2, p 207. (d) Boere, R. T.; Kidd, R. G. *Annu. Rep. NMR Spectrosc.* **1982**, *13*, 319.